Desalination and Water Treatment
www.deswater.com

doi: 10.1080/19443994.2016.1188732

57 (2016) 28964–28980
December

Taylor & Francis
Taylor & Francis Group

Adsorption removal of Methylene Blue (MB) dye from aqueous solution by bio-char prepared from *Eucalyptus sheathiana* bark: kinetic, equilibrium, mechanism, thermodynamic and process design

Sara. Dawood, Tushar Kanti Sen*, Chi Phan

Department of Chemical Engineering, Curtin University, GPO Box U1987, 6145 Perth, WA, Australia, email: sara.dawood@postgrad.curtin.edu.au (S. Dawood), Tel. +61 892669052; emails: t.sen@curtin.edu.au (T.K. Sen), c.phan@curtin.edu.au (C. Phan)

Received 3 February 2016; Accepted 7 May 2016

ABSTRACT

Eucalyptus bark (EB) materials-based bio-char adsorbent was synthesised and characterised using SEM-EDS, BET and CHN analyser. The adsorbent surface functional groups were determined by FT-IR analyser. Various textural characteristics such as BET surface area, pore size, bulk density, point of zero charge were also determined. The adsorption potential of these bio-char for the removal of cationic dye Methylene Blue (MB) from aqueous solution was studied. The effects of various temperature profiles on the production of EB bio-char were studied and the most efficient temperature profile was identified at 500˚C. Batch adsorption kinetic study showed that the amount of dye adsorbed q_t (mg/g) depends on various physicochemical process parameters such as initial solution pH, dye concentration, temperature, adsorbent dose, salt concentration and presence of SDS surfactant. It was found that the extent of MB dye adsorption by EB bio-char increased with the increase of initial dye concentration, contact time, temperature, SDS surfactant concentration and solution pH, but decreased with the increase of adsorbent dose and salt concentration. The optimum adsorption conditions were found at the initial dye concentration of 100 mg/L, initial solution pH of 11.3, adsorbent dose of 10 mg and solution temperature of 55˚C. Furthermore, pseudo-first-order, pseudo-second-order and intra-particle diffusion models were fitted to examine the adsorption kinetics and mechanism of adsorption. Equilibrium data were best represented by Langmuir isotherm model and gives a monolayer effective adsorption capacity of bio-char which is comparative to other adsorbents including commercial activated carbon. Thermodynamic parameters suggested that the adsorption was an endothermic, spontaneous and physical in nature. Furthermore, a single-stage batch adsorber design for the MB dye onto EB bio-char particles were presented based on the Langmuir isotherm model equation. These results indicated EB biomass as good and cheap precursor for the production of an effective and environmental friendly bio-char adsorbent.

Keywords: Eucalyptus bark-based bio-char; Methylene Blue dye; Adsorption; Isotherm; Kinetics

*Corresponding author.

1. Introduction

Dyes are complex organic compounds which are widely used in textile, printing, leather, cosmetic and paper industries and hence produce large amount of dye bearing liquid effluents. Effluent of such dye industries must be treated to bring down their concentration to a permissible limit before discharging into the water bodies [1]. Today, more than 100,000 commercial dyes are known with a total yearly production of 7×10^5 tonnes per year [2]. The high solubility of dyes in water effluents possesses serious risks to crop, aquatic life and human health [3]. Different separation techniques such as precipitation, ion-exchange, adsorption, coagulation/flocculation, advanced oxidation, ozonation, membrane separation and liquid–liquid extraction have been used to remove dyes from wastewater [4]. However, all the separation processes have their own advantages and disadvantages. Adsorption process is considered to be an effective separation technique compared to other available techniques for wastewater treatment in terms of cost, simplicity of design, high adsorption capacity and suitability to most toxic substances [5,6]. Commercial activated carbon (CAC) is widely used as an effective adsorbent in the removal of dyes and it is proven to be an effective adsorbent for the removal of variety of organic and inorganic pollutants dissolved in aqueous media or from gaseous environment [7]. However, many disadvantages are associated with this adsorbent including high cost, non-renewable production source and difficulties with its regeneration reuse gives reduction in adsorptive efficiency. Therefore, in the recent time, researchers are focusing upon the production of cost-effective naturally available agriculture solid waste-based adsorbents alternative to CAC. The applications of agricultural solid wastes as effective adsorbents offer several advantages. Their easy availability in large quantities, equipment of less processing time, renewable in nature, low cost, eco-friendly and good adsorption potential due to their unique chemical composition [2]. However, to produce effective high capacity adsorbents comparative to CAC, current research is also focusing on bio-char produced from various agricultural solid waste. Bio-char is a pyrogenic carbonaceous material produced from agricultural and forest residue by biomass carbonisation technology [8]. Generally, agriculture solid waste materials have little or no economic value and often present a disposal problem [9]. There are many reported agriculture solid waste-based bio-char and activated carbon used in the removal of various dyes such as Methylene Blue and Acid orange by bamboo bio-char [10], Reactive Violet by Cocoa shell activated carbon [11], Congo Red by pine cone-based activated carbon [12], Methylene Blue and Methylene Orange by Macore fruit activated carbon [13] and Acid Blue by waste tea activated carbon [14,15]. Readers are encouraged to go through these review articles.

Eucalyptus tree (*Eucalyptus sheathiana*) is naturally available in Australia and is cultivated as a street tree [3]. Eucalyptus bark (EB) is locally available with no economic value and therefore it was selected in this research project as a precursor for the production of cost-effective EB bio-char. The production of bio-char is considered to be more environmental friendly compared to activated carbon as it does not require any use of acids and bases. Eucalyptus bark is consisted of cellulose, hemicelluloses, tanning and lignin which is good for charcoal yield and adsorbents. Successfully raw Eucalyptus bark was used in the removal of Methylene Blue dye by adsorption [3]. However, raw Eucalyptus bark powder is considered a source of natural dye. Therefore, a new study is conducted on the removal of Methylene Blue dye using Eucalyptus bark-based bio-char to eliminate the release of the natural dye during adsorption process. In this work, the effectiveness of Eucalyptus bark (EB) biomass bio-char was prepared at 500˚C and characterised by Scanning Electron Microscopy with EDS (SEM-EDS), FTIR, BET, Malvern particle sizer, CHN analyser, bulk density and point of zero charge. Finally, its effectiveness in the removal of MB dye from its aqueous solution has been tested here by batch adsorption study, and various physicochemical process parameters have been identified and optimised. The mechanism of dye adsorption and kinetics has also been explored here. Further, great amount of salt and surfactant are utilised in the dying process and hence their presence in the liquid effluents may affect adsorption process and adsorbent capacity. Hence, salts and surfactant effects on MB dye adsorption gives further new aspects on this study.

2. Materials and methods

2.1. Raw material collection and preparation of agriculture solid waste bio-char

Eucalyptus barks (*E. sheathiana*) were collected from the Curtin University Bentley campus, Western Australia, Australia between February and March 2014. The barks were washed several times with ultrapure water to remove dust and impurities, dried at 75˚C for 24 h. The dried biomass was cut into small pieces with a maximum length of 10 cm and placed in a muffle furnace where temperature profile inside the muffle furnace was increased at the rate of 10˚C/min

until it reached the set point of 300, 400, 500, 600 and 700 °C, respectively, and kept at the set point temperature for a period of 2 h. The formed bio-char was cooled down at room temperature and then grounded using a mechanical grinder (manufactured by 135 RETSCH, GmbH & Co. KG, West Germany) and collected in a labelled plastic container.

2.2. Physical and chemical characterisation of EB bio-char

EB bio-char was characterised to determine the functional groups using a Spectrum 100 FT-IR spectrometer with a universal ATR sampling accessory with MIR detector from Perkin Elmer USA. Also, scanning electron microscope (SEM) (EVO 40) was used to study the morphological structure of the adsorbent's surface. The particle size was measured using Malvern Hydro 2000S Master Sizer (Malvern Instruments Ltd, UK). The surface area, and pore size of the adsorbent were determined using Brunauere–Emmett–Teller (BET) method by using Tristar II 3020 (Micromeritics Instrument Corporation). CHN analysis was conducted by CHN analyser to detect the amount of N_2, C and H_2 presented. Bulk density and bio-char yield were measured as per Eqs. (1) and (2), respectively:

$$\text{Bulk density} = \frac{\text{Mass of dry sample (g)}}{\text{Total volume used (ml)}} \quad (1)$$

$$\text{Yield } (\%) = \frac{w_c}{w_o} \times 100 \quad (2)$$

where w_c is the dry weight (g) of the final activated carbon and w_o is the dry weight (g) of precursor.

2.3. Chemicals

All chemicals used were of analytical grade. The cationic dye, Methylene Blue (MB) or methylthioninium chloride was selected as the adsorbate in the present study. It is a 3,7-bis (Dimethylamino)-phenothiazin-5-ium chloride with a formula: $C_{16}H_{18}N_3SCl$ and molecular weight of 319.85 g/mol. It was obtained from Sigma Aldrich with 99.9% purity. A stock solution of 1,000 mg/L was prepared by dissolving 1,000 mg powder of MB in 1,000 ml volumetric flask and filled it with ultra-pure water. Different experimental dye concentrations of 10, 20, 30, 40, 50 and 60 mg/L were prepared by diluting the stock solution with ultra-pure water. Also, sodium chloride and calcium chloride stock solutions were prepared by dissolving 1,000 mg salt powder in 1,000 ml volumetric flask and filled it with ultra-pure water. The pH of the solutions was adjusted by addition of either 1 M hydrochloric acid or 0.5 M sodium hydroxide solutions and measured using a digital pH meter (PHTESTR30). The SP-8001 UV/vis (V-670) spectrophotometer was used to measure the concentration of MB dye in solution where the maximum adsorption for the dye solution was measured at λ_{max} = 668 nm. The calibration curve was plotted between the absorbance and concentration of the dye solution to obtain the linear calibration equation. The concentration of the unknown solution was measured from the calibration plot.

2.4. Batch adsorption kinetic experiments

Adsorption measurements were determined by batch experiments of fixed amount of adsorbent with 50 ml of aqueous Methylene Blue dye solution of known concentration in a series of 125 ml plastic bottles. The mixture was shaken at a constant temperature using Thermo line scientific Orbital Shaker Incubator at 130 rpm at 35 °C temperature for 150 min. At predetermined time, the bottles were withdrawn from the shaker and the residual dye concentration in the reaction mixture was separated by centrifuging. Adsorption experiments were conducted by varying initial solution pH, contact time, adsorbent dose, initial dye concentration, initial salt concentration, initial SDS surfactant concentration and temperature. The amount of dye adsorbed onto EB bio-char at time t, q_t (mg/g) and % adsorption are calculated from Eqs. (3) and (4), respectively:

$$q_t = \frac{(C_0 - C_t)V}{m} \quad (3)$$

$$\%\ \text{Adsorption} = \frac{(C_0 - C_t)}{C_0} \times 100 \quad (4)$$

where C_0 is the initial dye concentration (mg/L), C_t is the concentration of dye at any time t, V is the volume of dye solution (0.05 L) and m is the mass of adsorbent in (g). All experimental measurements are within ±10% accuracy.

2.5. Isotherm experiment

Equilibrium adsorption studies were conducted by mixing 50 ml of dye solutions of various initial dye concentrations of 10, 20, 30, 40, 50, 70 and 100 mg/L

with 20 mg of EB bio-char powder in 125 ml plastic bottles for a period of 180 min which was more than sufficient to equilibrium time. The method is presented in Section 2.4.

3. Theory

3.1. Adsorption kinetic and mechanism

In order to investigate the mechanism of adsorption and the transient behaviour of the dye adsorption process, adsorption kinetics were studied and analysed using pseudo-first-order, pseudo-second-order and intra particles diffusion models as explained below.

3.1.1. Pseudo-first and pseudo-second-order models

Pseudo-first-order model was developed in 1898 [16]. The linearised forms of the pseudo-first-order and pseudo-second-order models are expressed as per Eqs. (5) and (6), respectively [4]:

$$\log(q_e - q_t) = \log q_e - \frac{k_F}{2.303}t \tag{5}$$

where q_t (mg/g) is the amount of dye adsorbed at time t, q_e (mg/g) is the adsorption capacity at equilibrium. The adsorption rate constant k_F (min^{-1}) and q_e (mg/g) were calculated from the slope and intercept of the linear plot of $\log(q_e - q_t)$ against (t).

$$\frac{t}{q_t} = \frac{1}{q_e}t + \frac{1}{k_s q_e^2} \tag{6}$$

The pseudo-second-order rate constant k_s (g/mg min) and q_e (mg/g) can be calculated from the slope and intercept of the linear plot (t/q_t) against (t).

3.1.2. Intra particles diffusion model

Intra-particle diffusion model is used for identifying the adsorption mechanism for design purpose [5]. For most adsorption processes, the amount of dye adsorbed varies almost proportionately with $t_{0.5}$ rather than with the contact time [9]. Where k_{id} (mg/g $min^{0.5}$) is the intra-particle diffusion rate constant and can be calculated from the slope of the linear equation of the plot q_t against $t^{0.5}$:

$$q_t = k_{id}t_{0.5} + C \tag{7}$$

3.2. Adsorption isotherm

Freundlich and Langmuir models were used to explain the MB dye-EB bio-char interaction relationship and to determine the adsorption capacity of adsorbent.

3.2.1. Freundlich isotherm

Freundlich model was developed to explain how adsorption takes place on heterogeneous surfaces [17]. In this study, Freundlich model was selected to explain MB dye and EB bio-char particles interaction relationship:

$$\ln q_e = \frac{1}{n}\ln C_e + \ln k_F \tag{8}$$

where q_e (mg/g) is the amount of dye adsorbed at equilibrium time, C_e is equilibrium concentration of dye in solution (mg/L). The Freundlich adsorption parameter, k_F and the heterogeneity factor ($1/n$) can be calculated from slope and intercept of the linear plot of $\ln q_e$ against $\ln C_e$. Also, if n value > 1, this indicates a favourable adsorption system.

3.2.2. Langmuir isotherm

Langmuir isotherm model was developed in 1916 [18] to explain how adsorption takes place on homogeneous surfaces. The linearised form of Langmuir model can be written as per Eq. (9):

$$\frac{C_e}{q_e} = \frac{1}{K_L q_e} + \frac{C_e}{q_m} \tag{9}$$

The maximum adsorption capacity q_m (mg/g) and Langmuir constant related to the energy of adsorption K_L (L/mg) were calculated from the slope and intercept of the linearised forms of the plots where (C_e/q_e vs. $1/q_e$). The separation factor (R_L) is a dimensionless used to investigate the adsorption system feasibility at different initial dye concentration and it can be calculated from Eq. (10):

$$R_L = \frac{1}{1 + K_L C_0} \tag{10}$$

where C_0 is the initial dye concentration (mg/L). Favourable adsorption process takes place where R_L value is $0 < R_L < 1$ [19].

3.3. Thermodynamic study

Thermodynamic studies have been investigated based on the equilibrium data. Gibb's free energy (ΔG°), enthalpy change (ΔH°) and change in entropy (ΔS°) were calculated by using the following equations [5,6], respectively:

$$\log \frac{q_e}{C_e} = \frac{\Delta S^\circ}{2.303\ R} + \frac{-\Delta H^\circ}{2.303\ RT} \quad (11)$$

$$\Delta G^\circ = \Delta H^\circ - T\Delta S^\circ \quad (12)$$

The linear form of the plot $\log(q_e/C_e)$ vs. $1/T$ presents Van't Hoff equation where q_e is the solid phase concentration at equilibrium (mg/L), C_e is equilibrium concentration in solution (mg/L), T is temperature in K and R is the gas constant (8.314 J/mol K). The enthalpy change (ΔH°) and change in entropy (ΔS°) values were calculated from the slope and intercept of the linear Van't Hoff plot $\log q_e/C_e$ vs. $1/T$.

4. Results and discussion

4.1. Characterisation of EB bio-char

4.1.1. Fourier-transform infrared (FTIR) spectrometer

Fourier-transform infrared (FTIR) spectrometer was used to investigate the functional groups presented in the EB bio-char before and after adsorption of MB dye as shown in Fig. 1. The absorption band at 3,500–3,300 cm^{-1} is presented with a peak band about 3,337 cm^{-1} and this is due to O–H vibrations of alcohols, phenols and carboxylic acids, as in cellulose and lignin [20]. Thus, phenolic and acidic groups are responsible for MB dye adsorption on EB bio-char.

N–H bending and stretching absorption bands are found at 11,607 cm^{-1} and 1,315 cm^{-1}. Also, a small peak of 2,162 cm^{-1} suggests the presence of C≡C stretching band. Another peak of 1,400 cm^{-1} is found and it suggests the presence of C–H scissoring and bending absorption band. C–N stretching is detected at the peak of 1,315 cm^{-1} where N–H bending band is detected at 900–650 cm^{-1} band. The FTIR analysis of EB bio-char after the adsorption of MB dye suggests the presence of N–H stretching band at 3,500–3,300 cm^{-1}. Also strong peaks of 1,592 and 1,387 cm^{-1} are noted which indicate the presence of C=C stretch aromatic ring and C–H scissoring and bending absorption bands, respectively. From Fig. 1, peaks such as 2,162 and 780 cm^{-1} of EB bio-char disappeared after the adsorption of MB dye while other peaks at 1,607 and 1,315 cm^{-1} shifted to 1,591 and 1,325 cm^{-1}, respectively, which suggest the aggregation of MB molecules with their functional groups of EB bio-char. Furthermore, a peak at 1,400 cm^{-1} has shifted to 1,387 cm^{-1} suggests that carboxyl group took part in the adsorption process. Also, the O–H stretching peak of 3,337 cm^{-1} has increased to 3,349 cm^{-1} after adsorption of MB dye which indicates significant hydrogen-bonding interaction in alkaline conditions.

4.1.2. Textural characteristics of EB bio-char

Textural characteristics of raw EB and EB bio-char are presented in Table 1. Table 1 shows that EB bio-char has higher specific surface area of 0.56 m^2/g, lower particle size of 10.68 μm and higher BET surface area compared to raw EB which may contribute to MB adsorption. Also, bulk density is an important parameter for consideration in the designing of pilot and commercial adsorption column. It is inversely related to the particle size of the adsorbent. The bulk density of raw EB and EB biomass-based bio-char were calculated as per Eq. (1). The American Water Work Association has set a lower limit on bulk density at 0.25 g/cm^3 for practical use. The bulk density of EB bio-char was calculated as 0.42 g/cm^3 which suggest the applicability of EB bio-char bulk density. Furthermore, the yield percentage of EB bio-char yield was calculated as per Eq. (2) as shown in Table 1. Where the pH_{pzc} of the EB bio-char was determined as per solid addition method [21] and it was found to be 9.5, signifying a positive surface charge for a solution pH below 9.5 and a negative surface charge for a pH greater than 9.5.

4.1.3. CHN analysis

CHN analysis was performed by CHNS-O analyser and the amount of N_2, C and H_2 presented in both raw EB and EB bio-char prepared under various temperature profiles are shown in Table 2. It was found that the amount of carbon increases from 40 to 60% for raw EB and EB bio-char (500°C), respectively, while the amount of hydrogen decreases from 5.4% to 1.68 for the same samples. However, the amount of nitrogen presence remains almost constant. Results obtained in this study are close to the reported results on C, H, N, element analysis with other biomass-based bio-char an activated carbon [12]. The amount of carbon and nitrogen contents of EB bio-char were higher compared to raw EB. The carbon prepared from EB has comparative properties and carbon content compared to commercial charcoal and bulk coal [22].

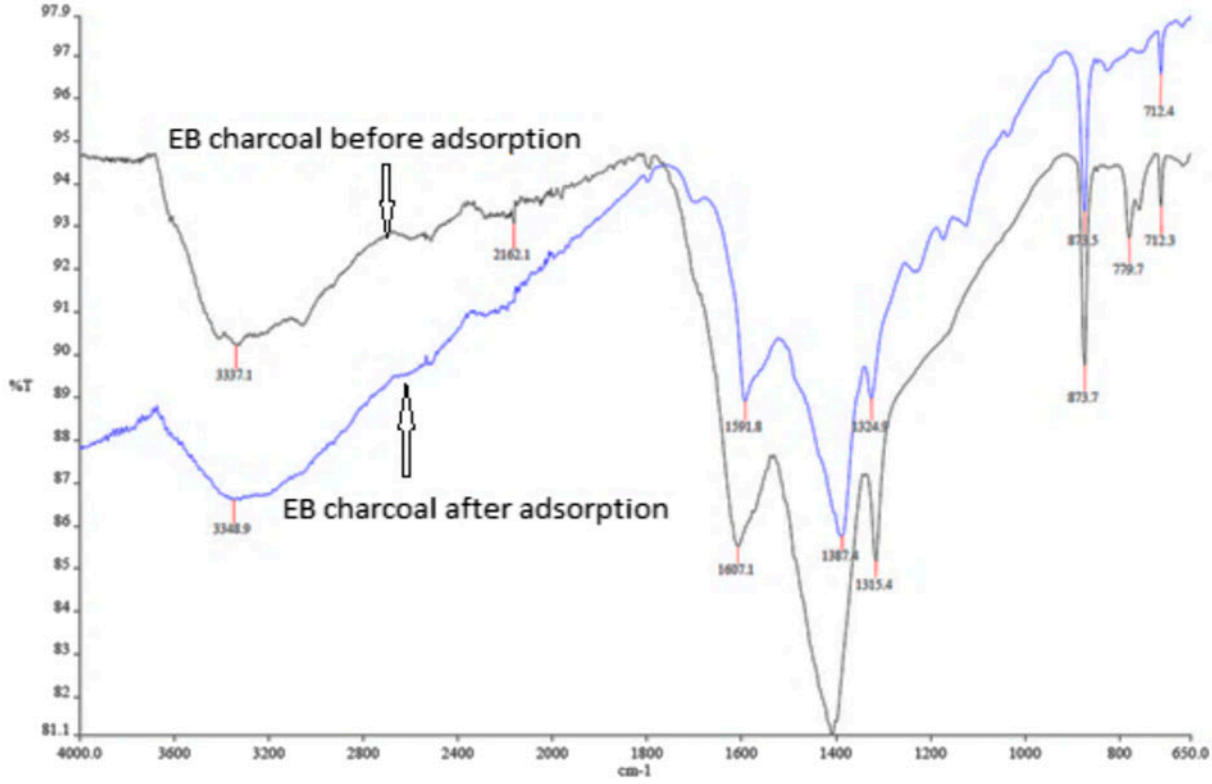

Fig. 1. FTIR of EB bio-char before and after the adsorption of MB dye.

Table 1
The textural characteristics of raw EB and EB bio-char

Characteristics	Raw EB	EB-based bio-char
BET surface area	6.2 m^2/g	73 m^2/g
Average pore size	18 Å	51 Å
Particle size	28.12 μm	10.68 μm
Specific surface area	0.20 m^2/g	0.56 m^2/g
Bulk density	0.35 g/cm^3	0.42 g/cm^3
Yield	–	36%
pH_{pzc}	5.0	9.5

Table 2
CHN analysis of raw EB and EB bio-char

Sample	C (%)	H_2 (%)	N_2 (%)
Raw EB	40.87	5.40	0.27
EB bio-char (300°C)	51.67	3.03	0.29
EB bio-char (400°C)	53.40	2.05	0.27
EB bio-char (500°C)	60.00	1.68	0.25
EB bio-char (600°C)	15.2 Ash	–	–
EB bio-char (700°C)	5.79 Ash	–	–
Commercial charcoal	73.6	3.17	1.4
Lignite coal	60–75	5.8–6	1.7–3.4

4.1.4. Scanning electron microscopy (SEM) analysis

The morphology of EB biomass-based bio-char before and after adsorption of MB dye is determined by scanning electron microscopy (SEM) as shown in Fig. 2(a) and (b), respectively. SEM micrograph of EB bio-char before adsorption shows a well-developed and heterogeneous structure with high porosity. The pores can be attributed to escaping volatiles during high temperature decomposition [8]. Upon the adsorption of MB dye, the porous structures are covered with uniform layer which should directly indicate the binding of MB dye into the surface of bio-char particles (Fig. 2(b)). As shown in Fig. 2(c), EB bio-char particles were analysed by energy dispersive X-ray spectroscopy (EDS) and it was found that carbon and oxygen were the main components however calcium may also presented in low proportion.

4.2. Effect of physicochemical process parameters on MB dye adsorption

4.2.1. Effect of initial solution pH

The solution pH affects the surface of adsorbent as well as the chemistry of the adsorbate and thus affects

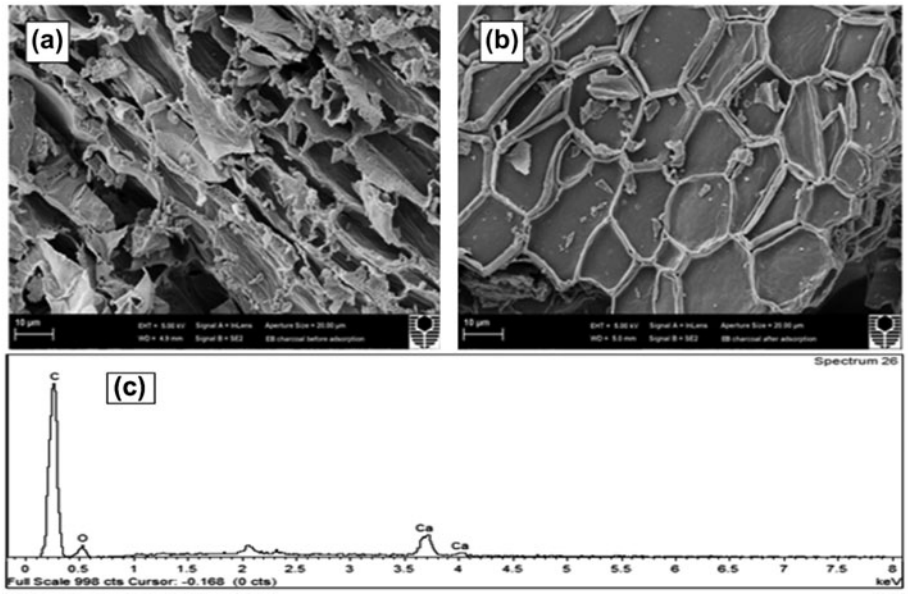

Fig. 2. SEM of EB bio-char (a) before adsorption of MB dye, (b) after adsorption of MB dye and (c) EDS of EB bio-char before adsorption.

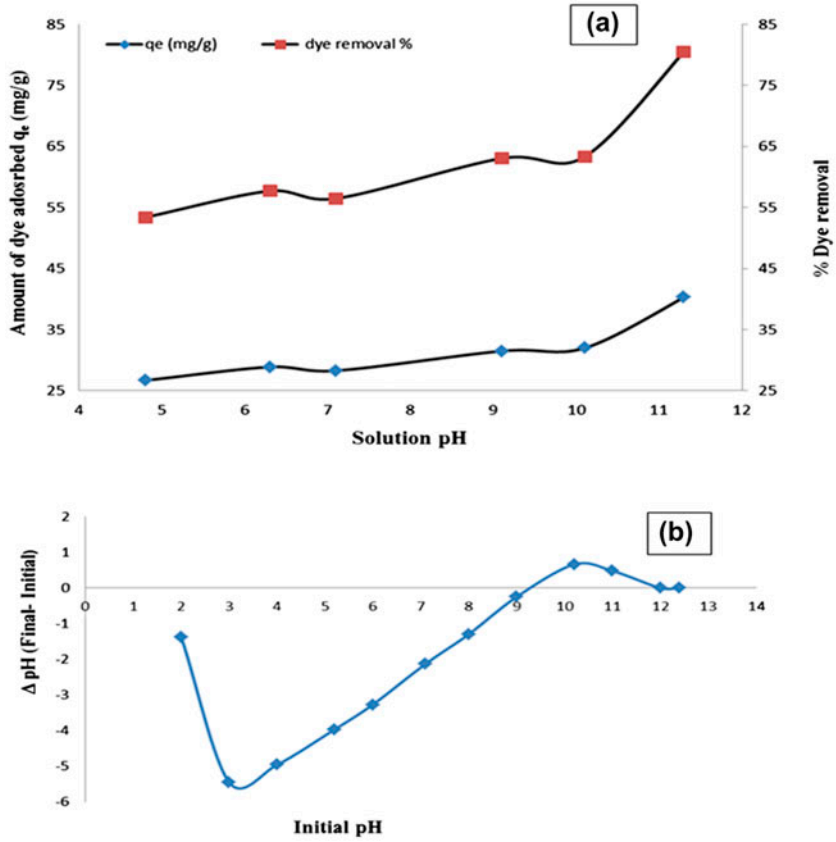

Fig. 3. (a) Effect of initial solution pH on the adsorption of MB dye onto EB bio-char: mass of adsorbent = 20 mg, volume of MB solution = 50 ml, initial dye concentration = 20 ppm, temperature = 35°C and shaker speed = 130 rpm and (b) the point of zero charge pH_{pzc} of EB bio-char.

the adsorption process. The effect of solution pH on the adsorption of MB dye from its aqueous solution by EB bio-char was studied in the range of 4.8–11.3 as shown in Fig. 3(a). It was found that the amount of dye adsorbed of MB dye, q_t (mg/g) is increasing from 26.7 to 40.3 mg/g with the increase of the solution pH as shown in Fig. 3(a). Also, it was found that the amount of dye removal efficiency increased from 53.4 to 80.5% due to increase in solution pH from 4.8 to 11.3 for a fixed initial dye concentration of 20 mg/L as per Fig. 3(a). To determine the point of zero charge, pH_{pzc} of EB bio-char, fixed amount of adsorbent was added to 50 ml of 0.1 M of KNO_3 solutions at various solution pH (2–12) as per solid addition method [21]. The point of zero charge (pH_{pzc}) of biomass-based bio-char in aqueous solution was determined as 9.5 from the plot of initial solution pH vs. $\Delta pH_{(final-initial)}$ as shown in Fig. 3(b). At pH values higher than the pH_{pzc} of 9.5, the EB bio-char adsorbent becomes more negatively charged due to dissociation of oxygenated group and formation of MB—oxygen binding sites takes place. In contrast, solution pH lower than pH_{pzc} of 9.5, the adsorbent becomes more positively charged. With the increase in solution pH, the number of negatively charged sites increases and hence it does favour for a cationic dye adsorption due to electrostatic attraction force. Lower solution acidic pH gives lower adsorption of MB dye which is due to presence of excess H^+ ions competing with the cationic group of dye for the adsorption sites. A similar behaviour was reported for MB dye adsorption on biomass and biomass-based carbon [2,4].

4.2.2. Effect of adsorbent dosage

The effectiveness of different doses of EB bio-char adsorbent on MB dye was studied to determine the most economical minimum dosage. It was observed that the increase in adsorbent dosage from 0.01 to 0.03 g results in decrease of amount of dye adsorbed (q_t) from 56.8 to 25.5 (mg/g) while the percentage dye removal is increasing from 56.8 to 80.5% as shown in Fig. 4. Fig. 4 shows the plot of the amount of MB dye adsorbed q_t (mg/g) and dye removal efficiency (%) against adsorbent concentration (mg) of EB bio-char. Initially, the rate of increase in the percentage of dye removal was found to be rapid and then slowed down as the dose increased. Furthermore, at dose of 20 mg, it was observed a slight decrease in the dye removal percentage of 80.5–76.6% compared to 30 mg adsorbent dose. This experiment was carried out at alkaline solution pH of 11.3 thus higher removal efficiency was observed. The decrease in amount of dye adsorbed q_t (mg/g) with increasing adsorbent mass is due to the split in the flux or the concentration gradient between solute concentration in the solution and the solute concentration in the surface of the adsorbent [12,23]. With the increase in adsorbent dose, the adsorption of MB dye on the adsorption surface was very fast which gives a lower adsorbate concentration in bulk solution compared to low adsorbent dose situation. Thus, with increasing adsorbent dose, the amount of dye per unit mass of adsorbent q_e (mg/g) decreased [24]. Whereas at low adsorbent dose, the adsorbate dye is more easily accessible and hence the dye removal per unit weigh of adsorbent is high. A similar behaviour is observed for MB dye adsorption on biomass and biomass-based carbon [3,15].

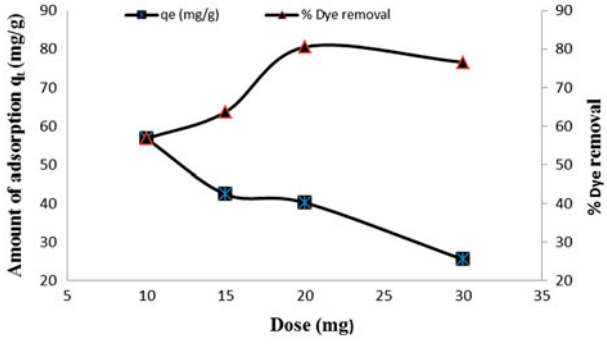

Fig. 4. Effect of adsorbent dosage of MB dye onto EB bio-char: pH solution = 11.3, volume of MB solution = 50 ml, initial dye concentration = 20 ppm, temperature = 35°C and shaker speed = 130 rpm.

4.2.3. Effect of contact time and initial Methylene Blue dye concentration

The initial dye concentration has a significant effect on its removal from aqueous solutions. The effects of various initial MB dye concentration and contact time on the adsorptive removal of dye by EB bio-char and raw EB were investigated and results are presented in Fig. 5(a) and (b), respectively. It was found that the amount of dye adsorbed q_t (mg/g) increased from 19.3 to 92.1 mg/g with increasing initial concentration of MB dye from 10 to 100 mg/L, respectively. The initial dye concentration provides a high driving force to overcome the resistance to the mass transfer of dye between the aqueous solution and the solid phase of a fixed adsorbent dose. Concurrently, the percentage of MB dye removal was decreased from almost 80.5 to 36.8% with increasing initial concentration of MB dye from 10 to 100 mg/L as shown in Fig. 5(a). Higher initial dye concentration causes the accumulation of dye molecules on the surface of the adsorbent particle which leads to the saturation of available active

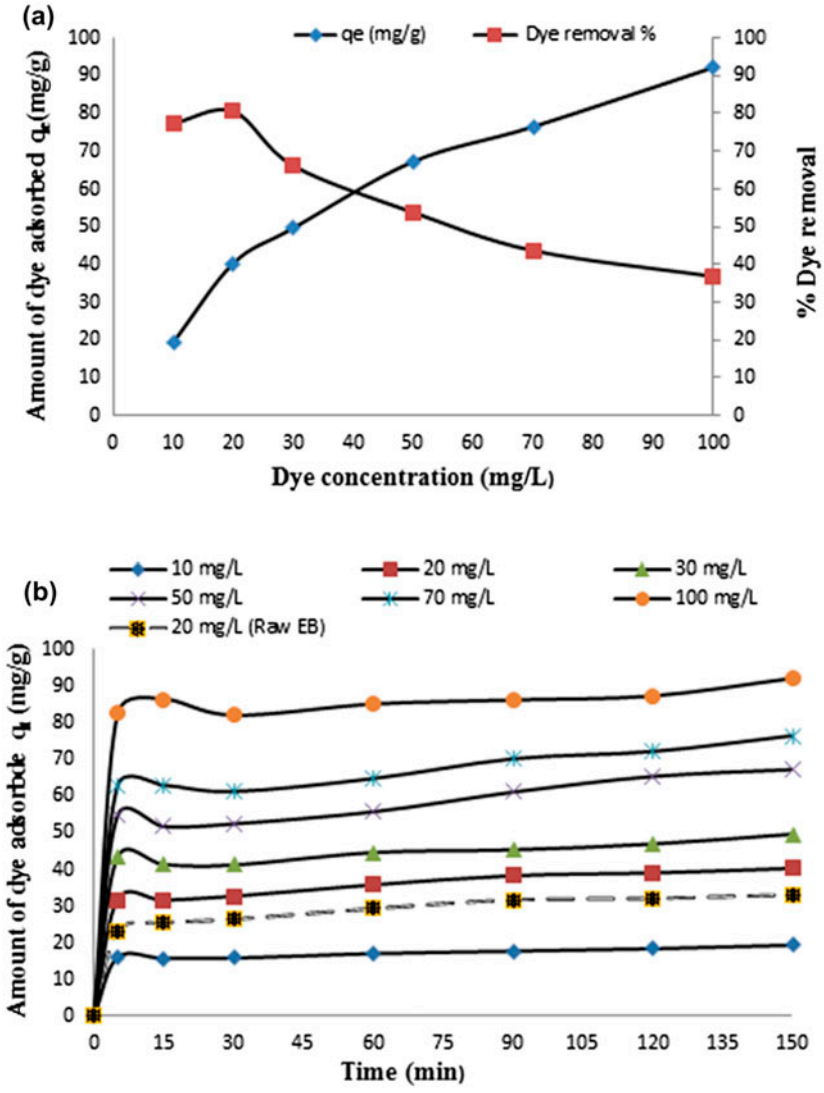

Fig. 5. (a) Effect of initial dye concentration of MB dye onto EB bio-char and (b) effect of contact time on MB dye adsorption onto raw EB and EB bio-char. Where pH solution = 11.3, volume of MB solution = 50 ml, initial dose = 20 mg, temperature = 35°C, shaker speed = 130 rpm and time (t) up to 150 min.

adsorption sites hence decreases the amount of dye removal [2]. It was also found that the amount of adsorption capacity q_t (mg/g) increases rapidly with increasing contact time at all initial dye concentrations and slowed down with the increases of contact time till equilibrium is attained within 150 min for both raw EB and EB bio-char adsorbents as shown in Fig. 5(b). Also, from Fig. 5(b), the amount of dye adsorbed q_t at equilibrium on raw EB and EB bio-char were calculated as 33.1 and 40.3 (mg/g), respectively, for an initial dye solution of 20 (mg/L). At this stage, the rate of adsorbed dye from adsorbent is in a state of dynamic equilibrium with the amount of dye being adsorbed on the surface of adsorbent and it also reflects the maximum adsorption capacity of an adsorbent under specific process conditions. A similar trend is reported by various research articles [2,4,5,9].

4.2.4. Effect of solution temperature and thermodynamics studies

The effect of different dye solution temperatures of 25, 35, 45 and 55°C on the adsorption kinetic was studied to determine the optimum solution temperature and the thermodynamic behaviour of MB dye adsorption on EB bio-char. That amount of MB dye adsorption on EB bio-char increased from 29.0 to 44.0 mg/g with increasing temperature of the solution

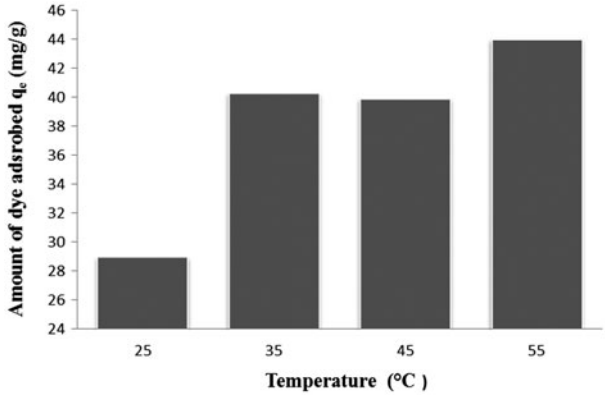

Fig. 6. Effect of temperature on MB dye adsorption onto EB bio-char: pH solution = 11.3, volume of MB solution = 50 ml, initial dose = 20 mg, initial dye concentration = 20 ppm, shaker speed = 130 rpm.

respectively as shown in Fig. 6. This trend indicates that the process is endothermic. This is also supported by thermodynamic parameter ΔG° which is decreasing with the increases of temperature as shown in Table 3. Generally, the ΔG° values is in the range of 0 to −20 kJ/mol indicates a physical adsorption [8]. The value of ΔG° at different temperatures indicates that the reaction was more favourable at higher temperature. This may be due to increase of active sites and also due to increase of the mobility of the dye molecules with increasing temperature [25]. This may also be due to increase in the pore size and activation of adsorbent surface. The thermodynamic parameters include Gibb's free energy (ΔG°), entropy (ΔS°) and enthalpy changes (ΔH°) were calculated as per Eqs. (11) and (12), respectively, and presented as per Table 3. The positive values of ΔH° and ΔS° indicate the endothermic nature and randomness at the solid solution interface occurs in the internal structure of the adsorption, respectively.

4.2.5. Effect of salts on Methylene Blue dye adsorption

Dye bearing effluents from textile industries contain significant amount of salts and hence the effect of salt on the adsorption process has to be considered. The presence of these salts in dye effluents affects both electrostatic and non-electrostatic interactions

Table 3
Thermodynamic parameters for adsorption of MB dye by EB bio-char

Temperature (K)	ΔG° (kJ/mol)	ΔH° (kJ/mol)	ΔS° (kJ/mol K)
298	−3.53	40.64	0.15
308	−5.01	40.64	0.15
318	−6.50	40.64	0.15
328	−7.98	40.64	0.15

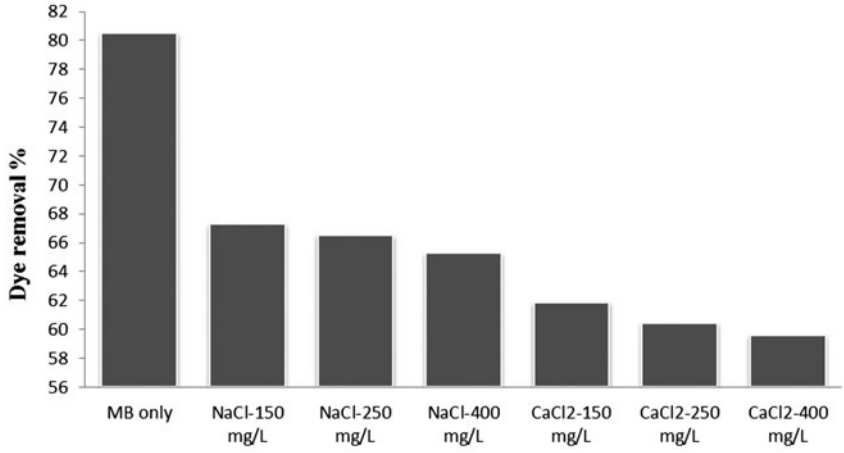

Fig. 7. Effect of sodium chloride and calcium chloride salts on MB dye adsorption onto EB bio-char, effect of pH solution = 11.3, volume of MB solution = 50 ml, initial dose = 20 mg, initial dye concentration = 20 ppm, shaker speed = 130 rpm.

between the adsorbent surface and dye molecules and therefore affects the adsorption capacity [3]. The effects of monovalent and divalent salts on the adsorption of MB dye have been examined using sodium chloride (NaCl) and calcium chloride ($CaCl_2$) salts, respectively. Kinetic experiments have been carried out by mixing initial salt concentrations of 150, 250 and 400 mg/L with MB dye solution at a fixed volume ratio of 1:9, respectively. It was found from Fig. 7, the amount of MB dye removal capacity was decreased due to the presence of monovalent NaCl and divalent $CaCl_2$ salts, respectively. Also, dye removal capacity was further slightly decreased upon the increase of initial NaCl and $CaCl_2$ salts concentration, respectively. It was observed that amount of dye removed was decreased from 67 to 60% upon the presence of fixed monovalent and divalent salt concentration, respectively. This trend indicates that the presence of external ionic strength in the aqueous solution could be attributed to the competitive effect between the cationic MB dye and the cations from the salts (Na^+ and Ca^{2+}) for the available active site which governs the adsorption process [26]. Also, the increase in the salt concentration (Na^+) may change the equilibrium constant between the interface and the bulk of the liquid thus affecting the adsorption operation. Similar trend was observed for divalent $CaCl_2$ salt. The molecular weight size, atomic radii and atomic charge of ions contribute significantly towards the efficiency of the adsorption process. Calcium ions have higher contribution to ionic strength and positive charge compared to sodium ions and hence the effect of Ca^{2+} ions on adsorption process is more serious than Na^+. Similar trend is reported by various research articles [6,24].

4.2.6. Effect of SDS surfactant on Methylene Blue dye adsorption

Sodium dodecyl sulphate (SDS) surfactant is an anionic organic compound and it is widely used as a stabilizer surfactant in textile industry and laundry cleaning products [27]. In order to estimate the effect of surfactant on MB dye adsorption, SDS surfactant with initial concentration of 20, 50 and 100 mg/L were mixed with MB dye solution at a volume ratio of 1:9, respectively, and other parameters were kept constant as per section 2.4. Results indicate that anionic surfactant SDS had a significant suppressing effect on the removal of dye MB. The amount of dye removal is decreased dramatically from 83 to 54% with the decrease of the surfactant concentration from 100 to 20 mg/L, respectively, for which the plot is not presented here. This trend can be explained based on known properties of the dye–surfactant aggregation system in the aqueous medium. It is known that ions from the cationic dye pairs with oppositely charged surfactants in which charges of the dye and the surfactant are compensated and can be retained on the nonpolar part of the sorbent. Also, high SDS concentration enhances conversion of hydrophilic MB dye into its respective hydrophobic ionic-pair concentration by displacing the equilibrium in the direction of MB–SDS formation [28] where at lower SDS concentration, this convention is not favourable.

4.3. Adsorption kinetic and mechanism of adsorption

4.3.1. Pseudo-first-order and pseudo-second-order kinetic models

Analysing the batch adsorption kinetics experiments play a major role in the designing, optimisation and production of industrial adsorption columns. The nature of the adsorption process depends on physical and chemical characteristics of the adsorbent system and also on the system conditions [5]. The applicability of pseudo-first-order and pseudo-second-order models were tested to investigate the adsorption nature of MB dye on EB bio-char as per Eqs. (5) and (6), respectively. Moreover, Chi-square (χ^2) test was performed to evaluate the accuracy of this kinetic model and determine the error between experimental ($q_{e)}$ and calculated (q_e) as shown in Eq. (14) [29]. Pseudo-first-order linear regression coefficient (R^2) values were calculated in the range of 0.64–0.84 for which

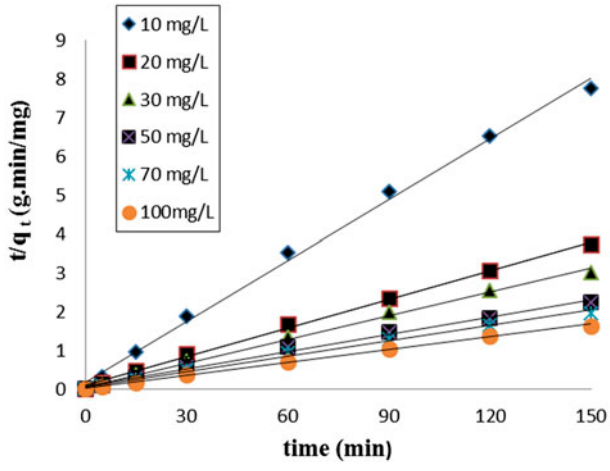

Fig. 8. Pseudo-second-order plot for initial adsorbent dose of EB bio-char onto MB dye: pH solution = 11.3, volume of MB solution = 50 ml, initial dose = 20 mg, temperature = 35°C, shaker speed = 130 rpm.

Table 4
Pseudo-second-order model parameters for adsorption of MB dye on EB bio-char

System parameters	q_e (mg/g), experimental	k_s (g/mg min)	q_e (mg/g), calculated	h (mg/g min)	χ^2	R^2
Adsorbent dosage (mg)						
10	56.8	0.004	56.5	14.0	0.001	0.996
15	42.5	0.005	42.9	8.5	0.005	0.996
20	40.3	0.007	40.3	10.9	0.000	0.997
30	25.5	0.013	25.1	8.2	0.009	0.996
Initial dye concentration (mg/L)						
10	19.3	0.015	19.1	5.5	0.002	0.996
20	40.3	0.007	40.3	10.9	0.000	0.996
30	49.6	0.007	48.8	16.2	0.014	0.997
50	67.2	0.003	67.1	13.8	0.000	0.996
70	76.5	0.003	75.2	19.3	0.021	0.995
100	92.1	0.006	90.1	52.6	0.045	0.998
pH						
11.3	40.3	0.007	40.3	10.9	0.000	0.997
10.1	30.2	0.020	29.6	18.0	0.005	0.999
9.1	31.9	0.008	31.8	8.2	0.001	0.996
7.4	28.2	0.011	28.5	9.1	0.002	0.998
6.3	28.9	0.009	28.7	7.5	0.001	0.995
4.8	26.7	0.017	26.7	12.5	0.000	0.999
Temperature (°C)						
25	28.9	0.013	27.6	9.5	0.063	0.997
35	40.2	0.007	40.3	10.9	0.000	0.996
45	39.9	0.004	40.3	6.1	0.005	0.998
55C	44.0	0.003	43.9	5.9	0.000	0.995
Monovalent salt-sodium chloride (mg/L)						
150	33.6	0.015	33.1	16.0	0.008	0.998
250	33.2	0.020	32.8	21.0	0.006	0.999
400	32.6	0.012	32.6	13.0	0.000	0.998
Divalent salt–calcium chloride (mg/L)						
150	30.9	0.015	31.1	14.8	0.002	0.999
250	30.2	0.009	30.1	8.3	0.000	0.996
400	29.8	0.018	30.3	16.3	0.008	0.999
SDS (mg/L)						
20	27.9	0.008	28.0	6.0	0.000	0.995
50	29.7	0.020	30.0	17.8	0.001	0.999
100	41.2	0.020	40.6	5.9	0.008	0.982

the plot is not presented here. The calculated (q_e) values were significantly lower than the experimental equilibrium adsorption capacity (q_e). Also, chi square test results with high error values which indicates the inapplicability of this model. Pseudo-second-order model was fitted where the (q_e) calculated values were almost identical to the experimental values. The (q_e) calculated values were obtained from the slope of the linearised form of the plot (t/q_t) vs. time (t). An example of pseudo-second-order kinetic plot fitting with experimental data for varying initial adsorbent dose is shown in Fig. 8. All the fitting kinetic parameters with various physiochemical process parameters are tabulated in Table 4. Pseudo-second-order rate constant k_s (g/mg min) decreased with the increase of dye concentration (Table 4). This may be due to the lower competition for the sorption sites at lower concentration. At higher dye concentrations,

the competition for the surface active sites will be high and hence lower adsorption rates are attained (Table 4). Whereas the initial adsorption rate h (mg/g min) was calculated as per Eq. (13) and it varied with adsorbent dose where the overall rate constant increased with the adsorbent dose. Also, from Table 4, the linear regression coefficients (R^2) values were above 0.97 and Chi square (χ^2) values were lower than 0.045 which suggested the applicability of this model. It was observed from Table 4, the adsorption capacity increases with the increase in initial dye concentration, solution pH and temperature but decreases with the increase of amount of adsorbent. Similar types of adsorption kinetic parameters were reported for the removal of MB dye by different [3,14]:

$$h = k \cdot q_e^2 \tag{13}$$

$$\chi^2 = \frac{\left(q_{e,exp} - q_{e,calc}\right)^2}{q_{e,calc}} \tag{14}$$

4.3.2. Intra particles diffusion model and mechanisms

Intra-particle diffusion model is used for identifying the adsorption mechanism that results in the apparent dynamic behaviour of the adsorption system. The most commonly used technique for identifying the mechanism involved in the sorption process is presented by fitting the experimental data onto intra-particle diffusion model as per Eq. (7). Intra-particle adsorption process is consisted of multi steps where migration of the dye molecules from the bulk solution to the surface of the sorbent, diffusion through the boundary layer to the surface of the sorbent, adsorption at sites and intra-particle diffusion into the interior of the sorbent [30]. It was found that the removal of MB dye by EB bio-char adsorbent was rapid at the initial period of contact time and then became slow and almost stable with the increases in contact time. This trend indicates the multistage of adsorption where the MB dye solution is adsorbed due to the external mass transfer followed by intra particle diffusion, respectively [6,31]. The overall rate of adsorption is controlled by the slowest step, which may be either film diffusion or pore diffusion. Also, from Eq. (7), the plots of q_t against $t_{0.5}$ give two or more intercepting lines depending on the actual mechanism where none of these plots give linear straight line segment passing through the origin. This trend shows that both film diffusion and intra-particle diffusion occurred simultaneously and the adsorption of MB dye onto EB bio-char particles may be controlled by film diffusion at earlier stages. Intra-particle diffusion plots for different solution pH, adsorbent dosages, temperatures, initial dye concentration, presence of ions and SDS surfactant are given same trends for which plots are not presented here. The diffusion coefficient (D_P) (cm^2/s) depends on the surface properties of adsorbents and it was calculated from Eq. (15). The half-life ($t_{0.5}$) (s) was calculated as per Eq. (7) and (r_0) is the radius of the adsorbent particle (cm). The surface weighted mean diameter of EB bio-char particle was found as 10.68 μm (radius = 5.34 μm × 0.0001 cm = 0.000534 cm). The intra particle diffusion coefficient (D_P) (cm^2/s) was calculated as 4.1×10^{-11}, 3.8×10^{-11}, 4.7×10^{-11}, 2.9×10^{-11}, 3.7×10^{-11}, 8.3×10^{-11} cm^2/s for 10, 20, 30, 50, 70 and 100 mg/L, respectively. Values of pore diffusion rate constants were found to be in the range of 10^{-11} cm^2/s for all the adsorbent samples. Therefore, the pore diffusion in this study may be significant:

$$t_{0.5} = \frac{0.03 r_0^2}{D_P} \tag{15}$$

4.4. Adsorption equilibrium isotherm

The adsorption equilibrium isotherm explains the specific relationship between the concentration of adsorbate and its degree of accumulation onto adsorbent surface at constant temperature [32]. The adsorbent surface phase may be considered as a monolayer or multilayer. Various isotherm models have been employed to fit the experimental data and evaluate the applicability of these models for MB dye adsorption. Freundlich and Langmuir models were used as per Eqs. (8) and (9), respectively. Langmuir isotherm is valid for monolayer adsorption on the adsorbent surface a finite number of identical sites while

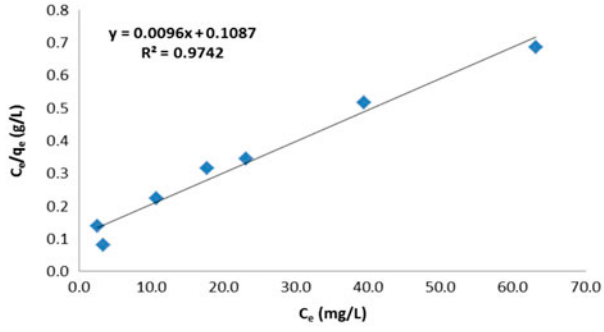

Fig. 9. Langmuir plot: for initial adsorbent dose of EB bio-char onto MB dye: pH solution = 11.3, volume of MB solution 50 ml, initial dose = 20 mg, temperature = 35°C, shaker speed = 130 rpm and time (t) = 180 min.

Table 5
A summary of Freundlich and Langmuir isotherm calculated values

Freundlich			
k_F (L/g)	n		R^2
17.99	2.48		0.848
Langmuir			
q_m (mg/g)	K_L (L/g)	R_L	R^2
104.17	0.09	0.1–0.4	0.974

Freundlich isotherm model is valid for multilayer adsorption and is derived by assuming a heterogeneous surface with interaction between adsorbed molecules with a non-uniform distribution of heat of sorption over the surface [6]. From the calculated date as shown in Fig. 9, it was found that Langmuir isotherm fitting for EB bio-char adsorbent gives a high linear regression coefficient (R^2) of 0.97 compared to 0.85 for Freundlich isotherm model which are presented in Table 5. High linear regression coefficient (R^2) indicates the applicability of Langmuir isotherm. From Table 5, the maximum adsorption capacity $q_m = 104.2$ mg/g and $K_L = 0.09$ values for Langmuir constants were obtained. Also, the constant value R_L (low separation factor) in Langmuir isotherm and Freundlich constant, n, were both presented in Table 5 and indicate a favourable and physical adsorption process. The Langmuir adsorption isotherm model provides the best fit for the system of EB bio-char adsorption on MB dye and similar adsorption isotherm trends were reported by various [3,4,14]. The adsorption capacity of EB bio-char into MB dye has been compared with other agriculture solid waste bio-char, biomass activated carbon and CAC under similar experimental conditions as presented in Table 6. From Table 6, it shows that EB bio-char studied in this work has a comparative adsorption capacity compared to other biomass carbon and activated carbon.

4.5. Design of single stage batch adsorber from isotherm data

It was found that Langmuir isotherm model is fitted well with the equilibrium data. Adsorption isotherms can be used to predict the design of single batch adsorption system [6,12]. Due to lack of extensive experimental data, empirical design procedures based on a batch adsorption isotherm study is used to predict the optimum process parameter such as the adsorber size and performance.

The design objective was to decrease the initial MB initial dye concentration from C_0 to C_t (mg/L) for which total dye solution is V (L). The amount of added adsorbent was m (g) and the solute loading increases from q_0 (mg/g) to q_t (mg/g). The MB dye concentration on solid changes from $q_0 = 0$ to q_t due to added adsorbent into the system. The mass balance for the MB dye in the single-stage operation under equilibrium is presented as in Eq. (16). Langmuir adsorption isotherm data has been utilised in this study to design a single-stage batch adsorption system as per method developed by [33]. Rearranging Eqs. (9) and (16) thus can be written as per Eq. (17):

$$V(C_0 - C_e) = m(q_e - q_0) = mq_e \tag{16}$$

$$\frac{m}{V} = \frac{C_0 - C_e}{q_e} = \frac{C_0 - C_e}{q_m K_a C_e / 1 + K_a C_e} \tag{17}$$

Table 6
Comparison of adsorption capacities of various adsorbents for removal of MB dye

Adsorbents	q_{max} (mg/g)	Refs.
Diatomite-templated carbons	505	[35]
Palm tree activated carbon	128	[36]
Nut shell activated carbon	5.3	[37]
Bio-char ash	178	[38]
Wheat straw bio-char	12.03	[39]
Wood apple shell activated carbon	37	[40]
Kenaf fibre char	22.7	[42]
Macore fruit activated carbon	10.6	[13]
Waste tea activated carbon	402	[14]
Granular activated carbon	21.5	[41,42]
Powdered activated carbon	91	[42]
EB bio-char	104.2	Present study

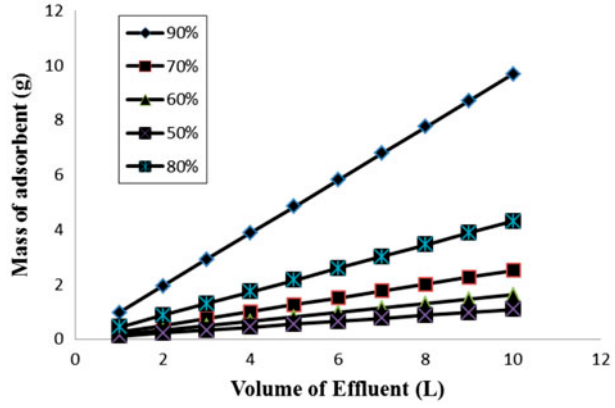

Fig. 10. Design of single stage batch adsorber—adsorbent mass (m) against volume of solution treated (L).

From Fig. 10, it shows a series of plots derived from Eq. (17) between the predicted amount of EB bio-char particles required to remove Methylene Blue dye of initial concentrations of 20 (mg/L) for 50, 60, 70, 80 and 90% dye removal at different solution volumes (L) for a single-stage batch adsorption.

4.6. Desorption study

Desorption studies has been performed to explain the adsorption mechanism and regeneration of the adsorbent. The MB loaded EB bio-char was separated from dye solution by centrifugation and dried. Fixed amount of 10 mg loaded dried adsorbent was agitated with 25 ml of acetone and distilled water at various pH values for predetermined equilibrium time of the adsorption process. It was found that the amount of dye regenerated increases with the decrease of solution pH for which the plot is not presented here. Desorption tests showed that amounts of dye released were 44, 43, 31, 30 and 28% achieved in aqueous solution at pH of 1.7, 2.3, 3, 5 and 11, respectively. The point of zero charge (pH_{pzc}) of EB bio-char was determined at solution pH of 9.5 therefore the amount MB dye released from the loaded EB bio-char is higher with the decrease of solution pH due to the enhanced electrostatic repulsion between the adsorbent and the adsorbate. Also, lower solution pH tends to give higher dye released percentage as the protons in solution replace the MB ions on the bio-char surface, while poor recovery of almost 28% is observed in high solution pH due to the coordinating ligands being deprotonated; hence, bound-dye ions find it difficult to be detached from the adsorbent [3]. Desorption of MB loaded EB bio-char at acidic solution pH indicates the adsorption process was through ion exchange. Also, it was found that the maximum dye releasing of 78% was achieved in an aqueous solution of acetone. Acetone is an organic compound that contains carbony1 groups which have both positive and negative centres and hence played the pivotal role in desorbing the adsorbed MB dye molecules from the EB bio-char sites [34]. Also, this result indicates the dye has been held by the adsorbent through a chemisorption process.

5. Conclusion

In the present study, eucalyptus barks bio-char was effectively used to remove Methylene Blue dye from aqueous solution. Agricultural by-product eucalyptus barks waste was considered as substance raw materials for the production of bio-char. The physical and chemical properties such as particle size, bulk density, carbon yield, BET surface area, CHN analysis, FT-IR and SEM of EB bio-char were also studied. It was found that the extent of MB dye adsorption by EB bio-char increased with the increasing of initial dye concentration, contact time, temperature, SDS surfactant concentration and solution pH, but decreased with the increase of adsorbent dose and salt concentration. Kinetic experiments clearly indicated that adsorption of Methylene Blue on EB bio-char are multi step processes: a rapid adsorption of dye onto the external surface followed by intra-particle diffusion into the interior of adsorbent which has also been confirmed by intra-particle diffusion model. Overall, the kinetic studies showed that the Methylene Blue dye adsorption process followed pseudo-second-order. Equilibrium data were fitted with Langmuir and Freundlich adsorption isotherm models. Based on the thermodynamic analysis and Langmuir isotherm data, it was observed that the adsorption system was endothermic and physical processes in nature. The positive value of ΔS° indicated also greater stability of an adsorption process with no structural changes at the solid–liquid interface. The present works also highlighted that eucalyptus barks bio-char is a good low-cost adsorbent in the removal of MB dye which has other applications. Further this biomass will add economic value and help to reduce the cost of agricultural solid waste disposal and provide a potentially inexpensive alternative adsorbent to CAC.

Acknowledgements

The Authors would like to thank the Chemical Engineering Department of Curtin University-Perth for providing research infrastructure. Also, the authors acknowledge the use of equipment and technical assistance of Electron Microscope Facility of Applied Physics department.

References

[1] G. Zhao, L. Jiang, Y. He, J. Li, H. Dong, X. Wang, W. Hu, Sulfonated graphene for persistent aromatic pollutant management, Adv. Mater. 23 (2011) 3959–3963.

[2] M.T. Yagub, T.K. Sen, S. Afroze, H.M. Ang, Dye and its removal from aqueous solution by adsorption: A review, Adv. Colloid Interface Sci. 209 (2014) 172–184.

[3] S. Afroze, T.K. Sen, M. Ang, H. Nishioka, Adsorption of methylene blue dye from aqueous solution by novel biomass *Eucalyptus sheathiana* bark: Equilibrium, kinetics, thermodynamics and mechanism, Desalin. Water Treat. 57 (2016) 5858–5878.

[4] S. Dawood, T.K. Sen, Review on dye removal from its aqueous solution into alternative cost effective and non-conventional adsorbents, J. Chem. Proc. Eng. 1 (2014) 1–7.

[5] S. Dawood, T.K. Sen, Removal of anionic dye Congo red from aqueous solution by raw pine and acid-treated pine cone powder as adsorbent: Equilibrium, thermodynamic, kinetics, mechanism and process design, Water Res. 46 (2012) 1933–1946.

[6] T.K. Sen, S. Afroze, H.M. Ang, Equilibrium, kinetics and mechanism of removal of Methylene Blue from aqueous solution by adsorption onto pine cone biomass of *Pinus radiata*, Water, Air, Soil Pollut. 218 (2011) 499–515.

[7] C.Y. Yin, M.K. Aroua, W.M.A.W. Daud, Review of modifications of activated carbon for enhancing contaminant uptakes from aqueous solutions, Sep. Purif. Technol. 52 (2007) 403–415.

[8] X. Hu, Z. Ding, A.R. Zimmerman, S. Wang, B. Gao, Batch and column sorption of arsenic onto iron-impregnated biochar synthesized through hydrolysis, Water Res. 68 (2015) 206–216.

[9] M.M.A. EI-Latif, A.M. Ibrahim, M.F. EI-Kady, Adsorption equilibrium, kinetics and thermodynamics of methylene blue from aqueous solutions using biopolymer oak sawdust composite, J. Am. Sci. 6 (2010) 267–283.

[10] P. Liao, Z.M. Ismael, W. Zhang, S. Yuan, M. Tong, K. Wang, J. Bao, Adsorption of dyes from aqueous solutions by microwave modified bamboo charcoal, Chem. Eng. J. 195–196 (2012) 339–346.

[11] M.C. Ribas, M.A. Adebayo, L.D.T. Prola, E.C. Lima, R. Cataluña, L.A. Feris, M.J. Puchana-Rosero, F.M. Machado, F.A. Pavan, T. Calvete, Comparison of a homemade cocoa shell activated carbon with commercial activated carbon for the removal of reactive violet 5 dye from aqueous solutions, Chem. Eng. J. 248 (2014) 315–326.

[12] S. Dawood, T.K. Sen, C. Phan, Synthesis and characterisation of novel-activated carbon from waste biomass pine cone and its application in the removal of congo red dye from aqueous solution by adsorption, Water Air Soil Pollut. 225 (2014) 1–16.

[13] K.N. Aboua, Y.A. Yobouet, K.B. Yao, D.L. Goné, A. Trokourey, Investigation of dye adsorption onto activated carbon from the shells of Macoré fruit, J. Environ. Manage. 156 (2015) 10–14.

[14] L. Borah, M. Goswami, P. Phukan, Adsorption of methylene blue and eosin yellow using porous carbon prepared from tea waste: Adsorption equilibrium, kinetics and thermodynamics study, J. Environ. Chem. Eng. 3 (2015) 1018–1028.

[15] Y. Gokce, Z. Aktas, Nitric acid modification of activated carbon produced from waste tea and adsorption of methylene blue and phenol, Appl. Surf. Sci. 313 (2014) 352–359.

[16] S. Lagergren, Zur theorie der sogenannten adsorption geloster stoffe (About the theory of so-called adsorption of soluble substances), Kungliga Sevenska. Vetens. 24 (1898) 1–39.

[17] H.M.F. Freundlich, Over the adsorption in solution, J. Phys. Chem. 57 (1906) 385–470.

[18] I. Langmuir, The constitution and fundamental properties of solids and liquids. Part I. Solids, J. Am. Chem. Soc. 38 (1916) 2221–2295.

[19] S. Kaur, S. Rani, R.K. Mahajan, Adsorption kinetics for the removal of hazardous dye congo red by biowaste materials as adsorbents, J. Chem. 2013 (2013) 1–12.

[20] S. Liang, X. Guo, N. Feng, Q. Tian, Isotherms, kinetics and thermodynamic studies of adsorption of Cu^{2+} from aqueous solutions by Mg^{2+}/K^{+} type orange peel adsorbents, J. Hazard. Mater. 174 (2010) 756–762.

[21] S. Nawaz, H.N. Bhatti, T.H. Bokhari, S. Sadaf, Removal of Novacron Golden Yellow dye from aqueous solutions by low-cost agricultural waste: Batch and fixed bed study, Chem. Ecol. 30 (2014) 52–65.

[22] W.N.R.W. Isahak, M.W.M. Hisham, M.A. Yarmo, Highly porous carbon materials from biomass by chemical and carbonization method: A comparison study, J. Chem. 2013 (2012) 1–6.

[23] V. Vadivelan, K.V. Kumar, Equilibrium, kinetics, mechanism and process design for the sorption of methylene blue onto rice husk, J. Colloid Interface Sci. 286 (2005) 90–100.

[24] R. Han, J. Zhang, P. Han, Y. Wang, Z. Zhao, M. Tang, Study of equilibrium, kinetic and thermodynamic parameters about methylene blue adsorption onto natural zeolite, Chem. Eng. J. 145 (2009) 496–504.

[25] M.A.M. Salleh, D.K. Mahmoud, W.A. Karim, A. Idris, Cationic and anionic dye adsorption by agricultural solid wastes: A comprehensive review, Desalination 280 (2011) 1–13.

[26] W.H. Li, Q.Y. Yue, B.Y. Gao, Z.H. Ma, Y.J. Li, H.X. Zhao, Preparation and utilization of sludge-based activated carbon for the adsorption of dyes from aqueous solutions, Chem. Eng. J. 171 (2011) 320–327.

[27] T.K. Sen, M.T. Thi, S. Afroze, C. Phan, M. Ang, Removal of anionic surfactant sodium dodecyl sulphate from aqueous solution by adsorption onto pine cone biomass of *Pinus radiate*: Equilibrium, thermodynamic, kinetics, mechanism and process design, Desalin. Water Treat. 45 (2012) 263–275.

[28] E.E. Baldez, N.F. Robaina, R.J. Cassella, Employment of polyurethane foam for the adsorption of Methylene Blue in aqueous medium, J. Hazard. Mater. 159 (2008) 580–586.

[29] E.H. Ezechi, S.R.b.M. Kutty, A. Malakahmad, M.H. Isa, Characterization and optimization of effluent dye removal using a new low cost adsorbent: Equilibrium, kinetics and thermodynamic study, Process Saf. Environ. Prot. 98 (2015) 16–32.

[30] W. Konicki, D. Sibera, E. Mijowska, Z. Lendzion-Bieluń, U. Narkiewicz, Equilibrium and kinetic studies on acid dye Acid Red 88 adsorption by magnetic $ZnFe_2O_4$ spinel ferrite nanoparticles, J. Colloid Interface Sci. 398 (2013) 152–160.

[31] F. Arias, T.K. Sen, Removal of zinc metal ion (Zn^{2+}) from its aqueous solution by kaolin clay mineral: A kinetic and equilibrium study, Colloids Surf., A 348 (2009) 100–108.
[32] X. Liu, L. Zhang, Removal of phosphate anions using the modified chitosan beads: Adsorption kinetic, isotherm and mechanism studies, Powder Technol. 277 (2015) 112–119.
[33] P. Senthil Kumar, S. Ramalingam, C. Senthamarai, M. Niranjanaa, P. Vijayalakshmi, S. Sivanesan, Adsorption of dye from aqueous solution by cashew nut shell: Studies on equilibrium isotherm, kinetics and thermodynamics of interactions, Desalination 261 (2010) 52–60.
[34] A.K. Chowdhury, A.D. Sarkar, A. Bandyopadhyay, Rice husk ash as a low cost adsorbent for the removal of Methylene Blue and congo red in Aqueous phases, Clean 37 (2009) 581–591.
[35] D. Liu, W. Yuan, P. Yuan, W. Yu, D. Tan, H. Liu, H. He, Physical activation of diatomite-templated carbons and its effect on the adsorption of methylene blue (MB), Appl. Surf. Sci. 282 (2013) 838–843.
[36] Z.A. AlOthman, M.A. Habila, R. Ali, A. Abdel Ghafar, M.S. El-din Hassouna, Valorization of two waste streams into activated carbon and studying its adsorption kinetics, equilibrium isotherms and thermodynamics for methylene blue removal, Arabian J. Chem. 7 (2014) 1148–1158.
[37] S. Ragupathy, K. Raghu, P. Prabu, Synthesis and characterization of TiO_2 loaded cashew nut shell activated carbon and photocatalytic activity on BG and MB dyes under sunlight radiation, Spectrochim. Acta Part A Mol. Biomol. Spectrosc. 138 (2015) 314–320.
[38] İ. Özbay, U. Özdemir, B. Özbay, S. Veli, Kinetic, thermodynamic, and equilibrium studies for adsorption of azo reactive dye onto a novel waste adsorbent: Charcoal ash, Desalin. Water Treat. 51 (2013) 6091–6100.
[39] Y. Liu, X. Zhao, J. Li, D. Ma, R. Han, Characterization of bio-char from pyrolysis of wheat straw and its evaluation on methylene blue adsorption, Desalin. Water Treat. 46 (2012) 115–123.
[40] R. Malarvizhi, N. Sulochana, Sorption isotherm and kinetic studies of methylene blue uptake onto activated carbon prepared from wood apple shell, J. Environ. Prot. Sci. 2 (2008) 40–46.
[41] D.K. Mahmoud, M.A.M. Salleh, W.A.W.A. Karim, A. Idris, Z.Z. Abidin, Batch adsorption of basic dye using acid treated kenaf fibre char: Equilibrium, kinetic and thermodynamic studies, Chem. Eng. J. 181–182 (2012) 449–457.
[42] J. Yener, T. Kopac, G. Dogu, T. Dogu, Dynamic analysis of sorption of Methylene Blue dye on granular and powdered activated carbon, Chem. Eng. J. 144 (2008) 400–406.